arXiv:0908.2220v2 [nucl-th] 9 Apr 2010

Triton Photodisintegration with Effective Field Theory

H. Sadeghi[a,1,*], S. Bayegan[b]

[a]*Department of Physics, University of Arak, P.O.Box 38156-879, Arak, Iran.*
[b]*Department of Physics, University of Tehran, P.O.Box 14395-547, Tehran, Iran.*

Abstract

Effective field theory (EFT) has been recently used for the calculation of neutron-deuteron radiative capture at very low energies. We present here the use of EFT to calculate the two-body photodisintegration of the triton, considering the three-body force. The calculated cross section shows sharply rising from threshold to maximum about 0.88 mb at ~ 13 MeV and decreasing slightly to about 0.81 mb at ~ 19 MeV, in corresponding to the experimental results. Our results are in good agreement with the experimental data and the other modern realistic two- and three-nucleon forces AV18/UrbanaIX potential calculation.

Keywords: 21.45.+v, 25.10.+s, 25.20.-x, 27.10.+h
PACS: effective field theory; triton photodisintegration; three-body force; photo-nuclear reactions

1. Introduction

The total photodisintegration cross sections of the three-body nuclei are important quantities for understanding electromagnetic processes in nuclei. The three-nucleon systems involving nucleon-deuteron radiative capture and photodisintegration of ^{3}He and ^{3}H have been investigated in experimental and theoretical works over the past decades.

In the experimental investigations, a few measurements of triton photodisintegration have been done. More recently, including of the two- and three-body reactions, photodisintegration cross sections are measured at low energies [1]. Mono energetic photons are used and neutrons are detected, in this experiment. The obtained $^3H(\gamma,n)^2H$ cross section shows sharply rising from threshold to the maximum of 0.9 mb at ~ 12 MeV and decreasing only slightly to 0.8 mb at ~ 19 MeV. The results are the two-body breakup cross sections for ^{3}H [1]. The same shape for the ^{3}He cross section has been reported but with the lower magnitude.

During the past several years, different theoretical approaches have been used in order to investigate the cross sections of the nucleon-deuteron radiative capture and photodisintegration of ^{3}He and ^{3}H from the very low energy up to 100 MeV. The main aim of these theoretical studies has been the calculations of the bound state and scattering wave functions in order to be used in matrix elements of the electromagnetic current operators and ultimately testing the underlying two, three body interactions as well as currents with certain degree of complexity for the three-nucleon systems. In many theoretical treatments, by solving the three-nucleon Faddeev equations based on simple finite rank forces, it is found that the interacting three-nucleon continuum is crucial for understanding the process in three-body reactions [2]. Sandhas and his collaborators investigated many theoretical treatments of photo-effect in ^{3}H and ^{3}He three-nucleon systems by employing the realistic nucleon-nucleon forces exclusive process at 0-40 MeV energies[3, 4]. For covering a larger energy range, the inclusive two- and three-body breakup cross sections have been studied by Efros et al. [5]. Recently, the Bonn group used the modern nucleon-nucleon forces. In these works, the current was restricted to the dominant E_1 multipole [6] or to the E_1 and E_2 multipoles [7]. They compared the Faddeev approach and a hyperspherical harmonic expansion together with the Lorentz integral transform method using AV18 together with Urbana IX.

*Corresponding author
Email address: H-Sadeghi@araku.ac.ir (H. Sadeghi)
[1]Tel:+988614173400, Fax:+988614173406

For the *p*-*d* and *n*-*d* radiative capture, a magnetic dipole M1 transition is a dominant contribution at the very low energy, in the plane wave(Born)approximation [8]. In such investigations, the authors employed Faddeev calculations, with the inclusion of three-body forces and meson exchange current(MEC). More recently, a very good agreement reached with the calculation of the total three-nucleon photodisintegration cross section with two quite different approaches [9]. Rather detailed investigation of such processes has been performed by Viviani et al. [10]. Recent calculation using manifestly gauge invariant currents reduced the spread [11], but the result including three-body currents, 0.558 mb, still over-predicts the cross-section by 10%. The V_{UCOM} potential leads to a very similar description of the cross section as the AV18 interaction, considering the Urbana IX three-body force for photon energies $45 \leq \omega \leq 120$ MeV, while larger differences are found close to threshold [12].

During the last few years, nuclear pionless EFT has been applied to the two-, three-nucleon systems [13, 14, 15, 16, 17, 18, 19, 21] and recently developed pionless EFT is particularly suited to the high order precision calculation. A recent model independent neutron-proton radiative capture calculation has been done, using EFT to predict a theoretical uncertainty 1% for center of mass energies $E \leq 1MeV$ [22]. At these energies, which are relevant for big-bang nucleosynthesis, isovector magnetic transitions M_1 and isovector electric transitions E_1 give the dominant contributions. In past years, we have calculated the cross section of $nd \rightarrow {}^3H\gamma$ process [23, 24, 25]. No new three-nucleon forces are needed in order to achieve cutoff independent results of neutron-deuteron radiative capture process up to next-to-next-to leading order($\mathrm{N^2LO}$). The three body parameters will be fixed by the triton binding energy and Nd scattering length in the triton channel.

In this paper, we study the two-body photodisintegration of the triton $\gamma^3H \rightarrow nd$ using pionless EFT and insertion of the three-body force, up to $\mathrm{N^2LO}$. The evaluated cross section has been compared with experimental data and the total cross section of the three-nucleon photodisintegration calculation of the modern realistic two- and three-nucleon forces AV18/UrbanaIX potential models. Close agreement between the available experimental data and the calculated cross section is reached. We demonstrate convergence and cutoff independence order by order in the low energy expansion.

The paper is organized as follows: in Section 2, we briefly review theoretical framework for calculating the Faddeev integral equation, Lagrangians for the reaction involved in our consideration, the relevant diagrams, three-body forces and cutoffs dependence. Comparisons of our results with the corresponding experimental and theoretical data are given in Section 3. Summary and conclusions follow in Section 4.

2. Theoretical framework

In the present work we confine ourselves with the electric and magnetic dipole approximation for the transition operators. These transitions are known to make most of the total cross section at least for the low energy region where the pionless EFT theory is most reliable. The photodisintegration reaction, $\gamma^3H \rightarrow nd$, in these energies occur predominantly via electric and magnetic, specially electric-dipole transition. The triton photodisintegration cross section is then given by [9]:

$$\sigma_{\gamma^3H\rightarrow nd}(E_\gamma) = (2\pi)^2(\frac{e^2}{\hbar c})M(E_\gamma)E_\gamma, \tag{2.1}$$

where E_γ is the incident photon energy and $M(E_\gamma)$ will be calculated from electric- and magnetic-dipole transition amplitudes. These transition amplitudes have been prepared by considering of the Faddeev equation for final nd-scattering and for the initial triton bound state system to some order (e.g. LO, NLO and $\mathrm{N^2LO}$). We then take these Faddeev amplitudes and folded with the photon-interaction with nucleons when the photon kernel is expanded to the same order.

The Lagrangians relevant to photodisintegration of the triton can be divided into:

(a) Lagrangian that contributes to nucleon-deuteron scattering. The derivation of the integral equation describing neutron-deuteron systems has been discussed before, see e.g. [16, 26, 21, 24]. Only the results will be used here. Two mixed configuration in the three-nucleon system are exist. The spin-triplet auxiliary deuteron field D_t combines, depending on their spin directions, with the nucleon N to total quartet channel spin ($S = \frac{3}{2}$) or doublet channel($S = \frac{1}{2}$).

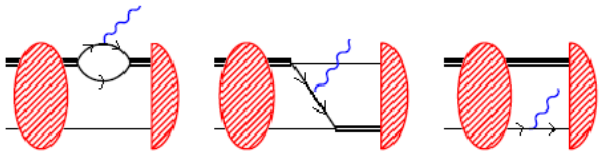

Figure 1: The Faddeev equation for Nd-scattering and diagrams for adding photon-interaction to the Faddeev equation contribution to E_1 amplitude.Wavy line shows photon and thick line is propagator of the two intermediate auxiliary fields D_s and D_t; $\mathcal{K}$: propagator of the exchanged nucleon, see eq.(2.2).

The Faddeev equation is introduced as a coupled equation and is given by [21]:

$$\begin{aligned}\begin{pmatrix} t^{(l)}_{d,tt} \\ t^{(l)}_{d,ts} \end{pmatrix}(E;k,p) &= 2\pi\, \mathcal{K}^{(l)}(E;k,p) \begin{pmatrix} 1 \\ -3 \end{pmatrix} \\ &- \frac{1}{\pi}\int_0^\infty \mathrm{d}q\, q^2\, \mathcal{K}^{(l)}(E;q,p) \begin{pmatrix} 1 & -3 \\ -3 & 1 \end{pmatrix} \begin{pmatrix} D_t(E-\frac{q^2}{2M},p) & 0 \\ 0 & D_s(E-\frac{q^2}{2M},p) \end{pmatrix} \begin{pmatrix} t^{(l)}_{d,tt} \\ t^{(l)}_{d,ts} \end{pmatrix}(E;k,q)\,,\end{aligned} \tag{2.2}$$

where $E := \frac{3\vec{k}^2}{4M} - \frac{\gamma^2}{M} - \mathrm{i}\epsilon$ is the total non-relativistic energy; the amplitude $t^{(l)}_{d,tt}$ for the $Nd_t \to Nd_t$-process; $t^{(l)}_{d,ts}$ for the $Nd_t \to Nd_s$-process; $\vec{k}$ the relative momentum of the incoming deuteron; $\vec{p}$ the off-shell momentum of the outgoing one, with $p = k$ the on-shell point; and the deuteron propagator only at LO is:

$$D(q_0,\vec{q}) = \frac{1}{\gamma - \sqrt{\frac{\vec{q}^2}{4} - Mq_0 - \mathrm{i}\epsilon}}. \tag{2.3}$$

The projected propagator of the exchanged particle on angular momentum l is given by:

$$\mathcal{K}^{(l)}(E;q,p) := \frac{1}{2}\int_{-1}^{1} \mathrm{d}x\, \frac{P_l(x)}{p^2+q^2-ME+pqx} = \frac{(-1)^l}{pq}\, Q_l\left(\frac{p^2+q^2-ME}{pq}\right), \tag{2.4}$$

where $Q_l(z)$, lth Legendre polynomial is:

$$Q_l(z) = \frac{1}{2}\int_{-1}^{1} \mathrm{d}t\, \frac{P_l(t)}{z-t}\,,$$

(b) Lagrangian that includes the new term generated by the two-derivative three-body force. Contrary to the terms without derivatives, there are different, inequivalent three-body force terms with two derivatives. But only one of them, H_2 is enhanced over its naive dimensional estimate, mandating its inclusion at N^{2}LO [18, 21].

In that case, a unique solution exists in the $^2S_{1/2}$-channel for each Λ and vanishing three-body force, but no unique limit as $\Lambda \to \infty$. As long distance, phenomena must however be insensitive to details of the short-distance physics (and in particular of the regulator chosen), Bedaque et al. [15, 16, 18, 26] showed that the system must be stabilized by introducing of a three-body force in a form:

$$\mathcal{H}(E;\Lambda) = \frac{2}{\Lambda^2}\sum_{n=0}^{\infty} H_{2n}(\Lambda)\left(\frac{ME+\gamma_t^2}{\Lambda^2}\right)^n. \tag{2.5}$$

which absorbs all dependence on the cutoff as $\Lambda \to \infty$ [18]. At leading order, $\gamma \ll \Lambda$, the essential observation are of order $O(Q/\Lambda)$ and are independent of energy (or momentum) and hence can be made to vanish by only H_0 and not any of the higher derivative three-body forces. At NLO, there is only a perturbative change from the LO asymptotic of order $O(1/\Lambda^2)$(see [18]).

For N^{2}LO order, a new three-body force seems to be required. The terms of order $(Q/\Lambda)^3$ is seems to be required, which guarantees that the amplitude is cutoff independent up to $(Q/\Lambda)^2$. The terms will be proportional to ME arising from expanding the kernel in powers of q/Λ and $\sqrt{ME}/\Lambda$ and a three-body force term which contains a dependence on the external momenta k^2 and ME can absorb them. It means we need H_2 for calculations up to N^{2}LO. It has been shown that the three body system at N^{2}LO can be renormalized without the need for an energy dependent three-body force at this order [20]. However, this work only discusses three-nucleon scattering at cutoffs, up to 500 MeV, that are large compared to the pion mass.

(c) Lagrangian that describing currents, contributing to $nd \to {}^3H\gamma$, which are not included in the previous two Lagrangians.

The polarization can be characterized by the three-vector $\vec{\epsilon}$, which satisfies the Lorentz condition: $\vec{\epsilon}\cdot\vec{k} = 0$, where $\hat{\vec{k}}$ is the unit vector along the photon three-momentum. The sum over the photon polarizations is given by:

$$\sum_{i=1,2} \epsilon_a^{(i)*}\epsilon_b^{(i)} = \delta_{ab} - \hat{k}_a\hat{k}_b,$$

where the upper index i numerates the two possible independent polarization vectors of the photon.

For photo production processes or radiative capture, the photon can be characterized by the smallest value of j. In this case, we can easily write the corresponding combinations of polarization $\vec{\epsilon}$ and unit vector $\hat{\vec{k}}$ for the photon states with low multipolarity:

$$\begin{aligned}
\vec{\epsilon} &\to E1 \text{ (electric dipole)},\\
\vec{\epsilon}\times\hat{\vec{k}} &\to M1 \text{ (magnetic dipole)},\\
\epsilon_a\hat{k}_b + \epsilon_b\hat{k}_a \equiv E_{ab} &\to E2 \text{ (electric quadrupole)},\\
(\vec{\epsilon}\times\vec{k})_a\hat{k}_b + (\vec{\epsilon}\times\vec{k})_b\hat{k}_a \equiv M_{ab} &\to M2 \text{ (magnetic quadrupole)}.
\end{aligned}$$

These are the basic formulas for the construction of the matrix elements for electromagnetic processes (in near threshold conditions). Main part of its contribution will be E_1 transitions for photon energies below 20 MeV. If the ground state of ${}^3H$ is thought to be an almost pure ${}^2S_{1/2}$ state, an electric-dipole transition gives a ${}^2P_{1/2,3/2}$ final state.

Cross sections for transitions to final states with isospin $T = 3/2$ correspond to the three-body breakup while those to $T = 1/2$ are known to correspond predominantly to the two-body breakup. The resulting matrix element for E_1 transition of $nd \to {}^3H\gamma$ process, can be written as:

$$(\vec{\epsilon}\cdot\vec{q})\ \left(t^\dagger\sigma_2\vec{\sigma}\ \cdot\vec{D}^*N\right), \tag{2.6}$$

where N, t, $\vec{q}$ and $\vec{D}$ are the 2-component spinors of initial nucleon, final ${}^3H$, the unit vector along the 3-momentum of the colliding nucleons and the polarization vector of the deuteron, respectively. The spin structure of the matrix elements for $N + d$ radiative capture is complicate also for the low energy interaction, as we have here 3 independent multipole transitions: $j^P = \frac{1}{2}^+ \to M1$ and $j^P = \frac{3}{2}^+ \to M_1$ and E_2. The following parametrization of the corresponding contributions to the matrix element are:

$$\begin{gathered}
i(t^\dagger N)(\vec{D}\cdot\vec{\epsilon^*}\times\vec{k}),\\
(t^\dagger\sigma_a N)(\vec{D}\times[\vec{\epsilon^*}\times\vec{k}])_a,\\
t^\dagger(\vec{\sigma}\cdot\vec{\epsilon^*}\,\vec{D}\cdot\vec{k} + \vec{\sigma}\cdot\vec{k}\,\vec{D}\cdot\vec{\epsilon}^*)N,
\end{gathered} \tag{2.7}$$

The first two structures in (2.7) are correspond to the M_1 radiation.

The E_1 and M_1 amplitudes receive contributions from the electric and magnetic moments of the nucleon and from four-nucleon operators coupling to the magnetic field, which are described by the two-body currents contributing to $nd \to {}^3H\gamma$ or ${}^3H\gamma \to nd$ [22]:

$$\mathcal{L}_{EM} = \frac{e}{2M_N} N^\dagger (k_0 + k_1\tau^3)\sigma.\mathbf{B}N + e\,L_B (N^T P_j N)^\dagger (N^T \overline{P}_3 N)\mathbf{B}_j$$
$$+\frac{1}{2} e\,L_E (N^T (\overleftarrow{\mathbf{D}}_j\, P_a^{(1)} - P_a^{(1)}\, \overrightarrow{\mathbf{D}}_j) N)^\dagger (N^T P_a N)\mathbf{E}_j + H.C. \tag{2.8}$$

where **E**, **B** and P_a are the electric, magnetic fields and the projector for the $^1S_0$ channel, respectively. The covariant derivative is:

$$D^\mu = \partial^\mu + ie\frac{1+\tau_3}{2}A^\mu \,,$$

and $P_i^{(1)}$ are the spin-isospin projectors for the isotriplet, spintriplet channel

$$P_i^{(1)} \equiv \frac{1}{\sqrt{8}}\sigma_2\sigma_i\,\tau_2\tau_3 \,, \qquad \mathrm{Tr}[P_i^{(1)} P_j^{(1)}] = \frac{1}{2}\delta_{ij}. \tag{2.9}$$

The L_B and L_E are determined from the two-body neutron-proton radiative capture and photodisintegration of the deuteron data, respectively, see [22] for more details.

The diagrams of E_1 contribution is shown in fig. 1. This figure shows simple inclusion of photon to the Faddeev equation contribution to E_1 amplitude. One of the other possible diagrams which could be contributed in the calculation is the insertion photon to exchanged nucleon(middle diagram in fig. 1). This diagram gives a tiny contribution when the photon couples electrically to exchanged nucleon, i.e. via $\vec{P}\cdot\vec{A}$. This is due to the fact that the initial and final state in this process are nearly orthogonal.

A higher dimension operator coupling an E_1 photon to a $^3S_1$-dibaryon and a p-wave two nucleon final state is suppressed by Q^3 in the power counting. This calculation involve only E_1 contribution. Meson exchange currents is another diagram to be incorporated and it is seen that electric quadrupole E_2 contributions are needed to achieve the better agreement between theory and experiment, specially at high energies. For higher energies, the present results are not complete and calculations with E_2 contribution must be carried out.

The M_1 amplitude receives contributions from the magnetic moments of the nucleon and dibaryon operators coupling to the magnetic field. Fig. 2 shows the diagrams for adding photon to the Faddeev equation up to N^{2}LO. There is no interaction of H_0 with a photon, because H_0 has no derivatives, so it is not affected by the minimal substitution $\vec{P} \to \vec{P} - e\vec{A}$. Contribution from the photon couples to the three-nucleon field (H_2) is not negligible(fig. 2) and should be calculated up to order of calculation. This coupling comes from the kinetic energy insertion of the three-nucleon field.

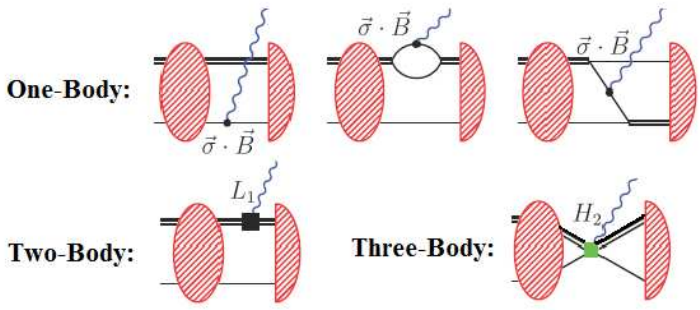

Figure 2: The Faddeev equation for *Nd*-scattering and some diagrams for adding photon-interaction to the Faddeev equation contribution to M_1 amplitude. The small circles show magnetic photon interaction. Vertices for photon interaction to two- and three-body system have been shown by L_1 and H_2, respectivly. Remaining notation as in fig. 1.

3. Results and discussion

The numerical calculations are done using $B = 2.225$ MeV ($\gamma_d = 45.7066$ MeV)for the NN triplet channel (deuteron binding momentum), $a_s = -23.714$fm for the NN singlet channel an ${}^1S_0$ scattering length. At LO and NLO, H_0 is the only three-body force entering and $H_2$is also required at N^{2}LO. The H_0 and H_2 three-body parameters are fixed from the ${}^2S_{\frac{1}{2}}$ scattering length $a_3 = (0.65 \pm 0.04)$ fm and the triton binding energy $B_3 = 8.48$ MeV, respectively. The L_B and L_E are obtained by fixing at leading non-vanishing order by the thermal neutron-proton radiative capture and deuteron photodisintegration cross sections, respectively [22].

In order to compute a solution, one introduces a cutoff Λ which is nonphysical and thus not to be confused with the breakdown scale $\Lambda_{\not\pi}$ of the EFT. We show cutoff variation of cross section between $\Lambda = 150$ MeV and $\Lambda = 500$ MeV as a function of the center of mass momentum is shown in fig. 3. A numerical investigation of the Faddeev equation confirms these findings. One can see smooth slope and does however change significantly from order to order, because the dominant correction is $(\gamma/\Lambda)^n$ and for these energy range at every order. These variations are nearly independent of variation of momentum. We confirm that, the cutoff variation decreases steadily as we increase the order of the calculation and it is of the order of $(k/\Lambda)^n, (\gamma/\Lambda)^n$, where n is the order of the calculation and $\Lambda = 150$ MeV is the smallest cutoff used. The other errors due to increasing momentum also appear in our calculation in low energy but these errors decrease when the order of calculation is increased up to N^{2}LO.

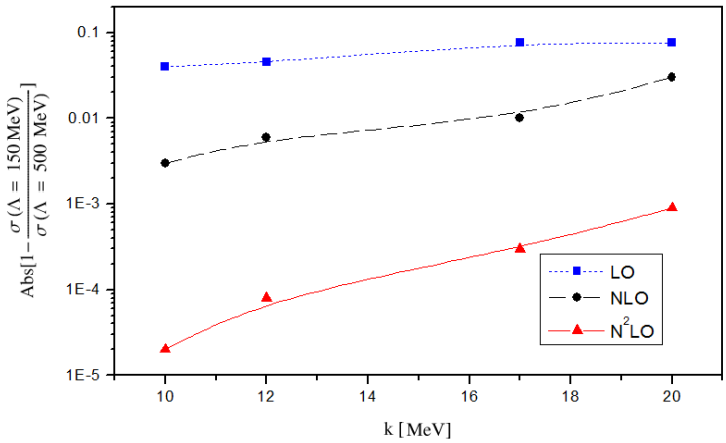

Figure 3: Curve of the cutoff variation of cross section up to N^{2}LO is shown between $\Lambda = 150$ MeV and $\Lambda = 500$ MeV. The short dashed, long dashed and solid line correspond to LO, NLO and N^{2}LO, respectively.

The breakdown of pionless EFT in calculation is estimated to be corresponds to photon energies of $m_\pi^2/M \approx 20$ MeV. The photodisintegration reaction $\gamma^3H \rightarrow nd$ results in the low photon energy range(0-20 MeV) are shown in table 1. It is well known that this reaction will be occurred predominantly via electric and magnetic, specially electric dipole transition. Our obtained results for electric dipole transition (E_1) show higher contribution in comparison with magnetic dipole transition (M_1) at these energies. The (E_1) contribution is calculated for LO and the next leading order is beyond N^{2}LO. The (M_1) contributions are calculated for LO, NLO and N^{2}LO. The calculated cross section shows sharply rising from threshold to maximum about 0.88 mb at ~13 MeV and decreasing only slightly to about 0.81 mb at ~19 MeV, in corresponding to experimental results [1].

In order to provide information on the dependence of the cross section calculation on the choice of models, forces and currents the results for the total two-body photodisintegration cross section of ^{3}H have been displayed at two energies in table 2. At 12 MeV, one can see a good agreement between the results of AV18 and UrbIX with three-nucleon forces and pionless EFT result up to N^{2}LO. It is also found, the two-body photodisintegration of the triton cross section is dominated by E_1 transition.

Comparison of the different models, show that the results of pionless EFT up to N^{2}LO are in good agreement with the other modern nucleon-nucleon potentials with three-nucleon forces. Table 2 illustrates also that the result with

E_γ (MeV)	$\sigma(M_1)$ (LO)	$\sigma(E_1)$ (LO)	$\sigma(M_1+E_1)$ (LO)	$\sigma(M_1)$ (NLO)	$\sigma(M_1+E_1)$ (NLO)	$\sigma(M_1)$ (N^2LO)	$\sigma(M_1+E_1)$ (N^2LO)	Exp. (mb)
11.54	0.039	0.782	0.821	0.054	0.833	0.063	0.845	0.84 ± 0.05
11.92	0.037	0.800	0.837	0.050	0.855	0.060	0.860	0.95 ± 0.05
12.55	0.034	0.820	0.854	0.045	0.870	0.055	0.875	0.96 ± 0.06
13.04	0.030	0.830	0.860	0.041	0.876	0.049	0.880	0.86 ± 0.05
13.92	0.027	0.831	0.858	0.038	0.874	0.047	0.878	0.79 ± 0.06
14.92	0.026	0.827	0.853	0.036	0.868	0.045	0.872	0.71 ± 0.06
15.92	0.023	0.820	0.843	0.033	0.858	0.042	0.862	0.61 ± 0.05
16.80	0.020	0.810	0.830	0.030	0.845	0.038	0.848	0.85 ± 0.06
17.66	0.018	0.796	0.814	0.027	0.828	0.035	0.835	0.74 ± 0.07
18.67	0.015	0.786	0.801	0.024	0.815	0.032	0.818	0.66 ± 0.07
19.16	0.014	0.778	0.792	0.022	0.805	0.030	0.808	0.66 ± 0.07
19.72	0.013	0.770	0.783	0.021	0.796	0.029	0.799	0.71 ± 0.11

Table 1: The cross section for $\gamma^3H \to nd$ in millibarns computed in pionless EFT up to N^{2}LO. The pionless EFT cross section is comprised of the E_1 amplitude computed to LO and the M1 amplitude computed to LO, NLO and N^{2}LO. The last column shows the experimental date from [1].

Type of Formulation	E_γ = 12 [MeV]	E_γ = 40 [MeV]
AV18-Siegert	1.056	0.168
AV18-MEC	0.949	0.155
CD Bonn2000-Siegert	0.980	0.169
AV18+UrbanaIX-Siegert	0.882	0.180
AV18+UrbanaIX-MEC	0.915	0.169
CDBonn2000+TM'-Siegert	0.889	0.176
EFT(N^{2}LO)	0.874	0.240

Table 2: The total cross section results(in mb) for two-body photodisintegration of ^3H of different models-dependent based on Faddeev approach [27]. The last row shows model-independent EFT result up to N^{2}LO.

explicit MEC differs rather substantially from that with the one-body current and implicit MEC via Siegert's theorem as well as EFT results. However, precise data would be required in order to reach a better conclusion.

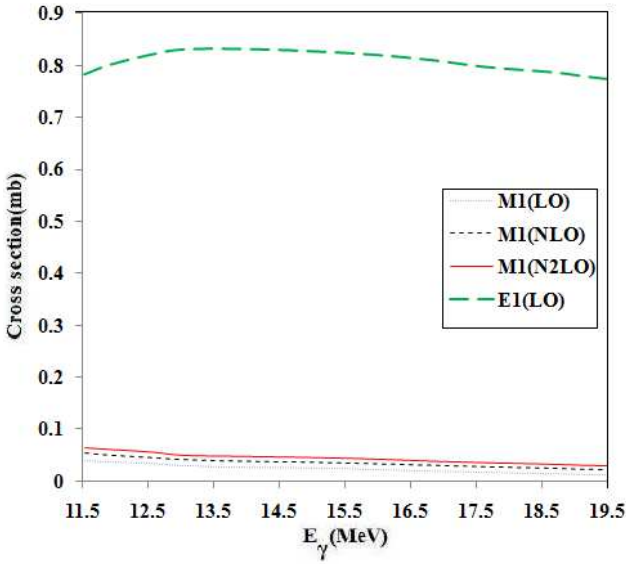

Figure 4: ^{3}H photo-dissociation cross section σ (mb) for center of mass energy E (MeV). Dot, dash and solid curve are LO, NLO, and N^{2}LO M_1 transitions,and long-dash is LO E_1 transition.

The leading contributions from each transitions are shown in fig. 4. One can see that the M_1 transition is small in comparisons to E_1 transitions and as a results the E_2 transitions can be ignored for calculation in the energy range of our interest. A comparison between the low energy cross section computed with pionless EFT and the experimental data as well as the potential model calculation, can be seen in fig. 5. A detailed and very illuminating discussion of the experiments that contributed to these data points can be found in ref. [1]. One finds a rather good agreement between pionless EFT theory and experiment at low energy. Since the experimental situation is not settled, a good definite comparison between theory and experiment cannot be made. It is due to the fact that the two-body break up data are rather scattered and there is also limited experimental information on the three-body break up.

We also compared the obtained total ^{3}H cross section with the other modern nucleon-nucleon AV18/UrbanaIX [27], in fig. 5. One finds a rather good agreement between EFT results up to N^{2}LO and the experimental data, as well as, potential models that the three-nucleon forces improve their consistency with the experiments. On the other hand, due to the insufficient precision of the experimental data a more conclusive comparison between theory and experiment cannot be made. As another result, we leave the consistency of our results for energies higher than $\sim$ 20 MeV. This is in agreement with the breakdown energy scale of pionless EFT ($\sim$ 20 MeV). Effects of others multipoles, retardation, tensor correlations, and subnuclear currents should have more and more influence at higher energies.

Our result using EFT is model independent and universal, any model with the same input must, within the accuracy of our calculation, lead to the same result. Due to the large error bars in experimental data, it is not possible to draw further conclusions.

4. Summery and conclusion

We calculated the cross section of photo-dissociation of $\gamma^3 H \rightarrow nd$. We applied EFT to find numerical results for this process. The results are compared with, AV18 together with the Urbana IX three-nucleon forces or CD Bonn with TM three-body forces, high precision other nuclear force models. Our results are in good agreement with the other calculations and experimental data. Theoretical predictions show the maxima sharply rising from threshold to maximum about 0.88 mb at $\sim$ 13 MeV and decreasing only slightly to about 0.81 mb at $\sim$19 MeV, in corresponding to experimental results.

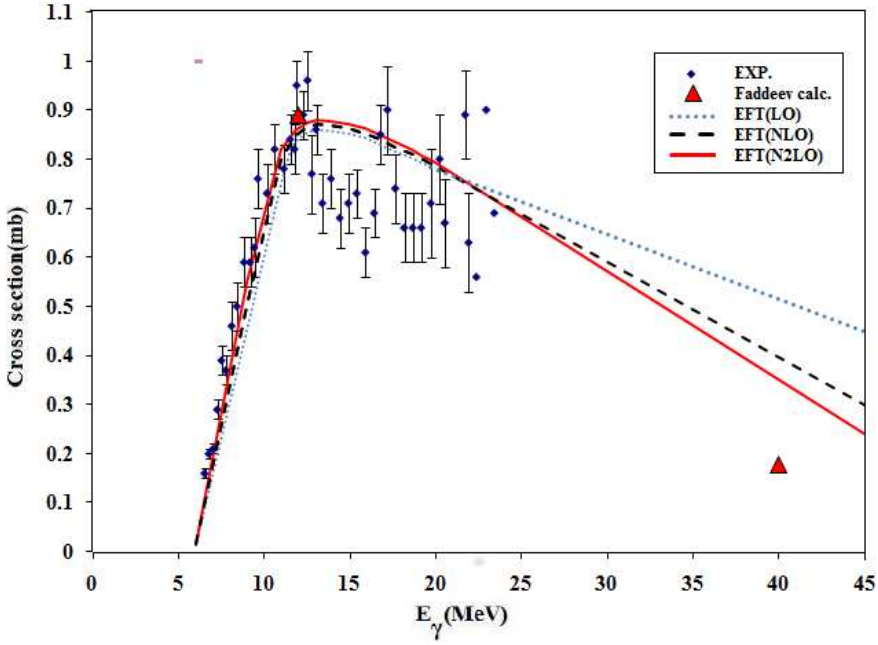

Figure 5: The cross section for $\gamma^3H \to nd$ near threshold, as a function of the incident photon energy in MeV. The solid curve corresponds to the cross section computed in pionless EFT up to N^{2}LO. The dotes with error bar correspond to the experimental date from [1] and triangle points show the Faddeev calculation results for cross sections of the ^{3}H photodisintegration [27]. The short dashed, long dashed and solid line correspond to LO, NLO and N^{2}LO effective field theory calculation, respectively.

The results are quantitatively supported by available data and converge order by order in low energy expansion. The results are also cutoff independent when the order of calculation is increased up to N^{2}LO. High quality experimental data would be very helpful more strongly to challenge theory at low energies.

5. Acknowledgments

The authors would like to thank Harald W. Grießhammer for useful and valuable comments.

[1] D.D. Faul, B.L. Berman, P. Meyer and D.L. Olsenp, Phys. Rev. C **24**, (1981) 849.
[2] I.M. Barbour and A.C. Phillips, Phys. Rev. C **1**, (1970) 165 .
[3] W. Schadow and Sandhas, Phys. Rev. C **55**, (1996) 1074.
[4] W. Schadow, O. Nohadani and Sandhas, Phys. Rev. C **63**, (2001) 044006.
[5] V.D. Efros, W. Leidemann, G. Orlandini and E.L. Tomusiak, Phys. Lett. B **484**, (2000) 223.
[6] W. Sandhas, W. Schadow, G. Ellerkmann, L.L.Howell and S.A.Sofianos, Nucl. Phys. A **631**, (1998) 210c.
[7] W. Schadow, O. Nohadani and W. Sandhas, Phys. Rev. C **63**, (2001) 044006.
[8] J.L. Friar, B.F. Gibson and G.L. Payne, Phys. Lett. B **251**, (1990) 11.
[9] J. Golak, R. Skibinski, W. Gloeckle, H. Kamada, A. Nogga, H. Witala, V. D. Efros, W. Leidemann, G. Orlandini and E.L. Tomusiak, Nucl. Phys. A **707**, (2002) 365.
[10] M. Viviani, R. Schiavilla and A. Kievsky, Phys. Rev. C **54**, (1996) 534.
[11] L.E. Marcucci, M. Viviani, R. Schiavilla, A. Kievsky and S. Rosati, Phys. Rev. C **72**, (2005) 014001.
[12] S. Bacca, Phys. Rev. C **75**, (2007) 044001.
[13] D. B. Kaplan, M. J. Savage and M. B. Wise, Nucl. Phys. B **534**, (1998) 329.
[14] S. R. Beane and M. J. Savage, Nucl. Phys. A **694**, (2001) 511.
[15] P. F. Bedaque, H.-W. Hammer and U. van Kolck, Phys. Rev. Lett. **82**, (1999) 463; Nucl. Phys. A **646**, (1999) 444.
[16] P. F. Bedaque, H.-W. Hammer and U. van Kolck, Nucl. Phys. A **676**, (2000) 357.
[17] H.-W. Hammer and T. Mehen, Phys. Lett. B **516**, (2001) 353.
[18] P. F. Bedaque, G. Rupak, H. W. Grießhammer and H.-W. Hammer, Nucl. Phys. A **714**, (2003) 589.
[19] F. Gabbiani, P. F. Bedaque and H. W. Grießhammer, Nucl. Phys. A **675**, (2000) 601.
[20] L. Platter and D. R. Phillips, Few Body Syst. **40**, (2006) 35.
[21] H.W. Grießhammer, Nucl. Phys. A **760**, (2005) 110.

[22] G. Rupak, Nucl. Phys. A **678**, (2000) 405.
[23] H. Sadeghi and S. Bayegan, Nucl. Phys. A **753**, (2005) 291.
[24] H. Sadeghi, S. Bayegan and H. W. Grießhammer, Phys. Lett. B **643**, (2006) 263.
[25] H. Sadeghi, Phys. Rev. C **75**, (2007) 044002.
[26] H. W. Grießhammer, Nucl. Phys. A **744**, (2004) 192.
[27] R. Skibinski, J. Golak, H. Kamada, H. Witala, W. Glockle and A. Nogga, Phys. Rev. C **67**, (2003) 054001.